Precipitation in a Cu-30 Pct Ni-1 Pct Nb Alloy

M. RAGHAVAN

Decomposition of a Cu-30 pct Ni-1 pct Nb alloy on aging in the range of 866 K (600°C) to 1073 K (800°C) was investigated. The initial decomposition, concomitant with age hardening, occurred through the precipitation of body centered tetragonal metastable Ni_3Nb-γ'' precipitates on the {100} matrix planes. Equilibrium orthorhombic β phase formed either through a grain boundary cellular reaction at low temperature (≤973 K (700°C)) or as Widmanstaetten platelets on the {111} planes at higher temperatures (≥1073 K (800°C)) with the following crystallographic relationship:

$(010)_\beta // (111)_\gamma$

$[100]_\beta // [1\bar{1}0]_\gamma$.

Based on the observations, a schematic transformation sequence is presented.

ENHANCEMENT in strength of nickel-base super alloys and iron-base alloys has been achieved through the precipitation of metastable γ''-Ni_3Nb and γ' precipitates.[1-13] The strengthening due to the γ'' precipitates in a nickel-base alloy has been discussed in detail by Oblak, *et al*[1] and Kirman and Warrington.[8,9] Except for the early work by C. S. Smith,[14,15] no attempts have been made to investigate the precipitation of γ''-Ni_3Nb precipitates in copper-base alloys and the potential strengthening that could be derived from these precipitates. Though the solid solubility of niobium in pure copper is limited at elevated temperature, C. S. Smith's work indicated enhanced solubility of Nb and Ta in Cu-Ni alloys. His work suggested that the solid solubility of Ta in a Cu-30 pct Ni alloy can be increased to 2.7 pct* at 1372 K (1100°C) and Nb could replace Ta totally or in part. Also, significant enhancement in room temperature strength and softening resistance was observed in the alloys containing Nb and Ta.

*Compositions refer to wt. pct.

Precipitation of ordered, coherent, Ni_3Nb (γ'') particles in nickel and iron base alloys is well understood.[1-11,16,17] These γ'' precipitates have a bct crystal structure with a c/a ratio of 2.04 and form as thin platelets on the cube planes of the matrix with the c axis of the bct unit cell normal to the platelets. The positive misfit between γ'' and γ is maximum normal to the platelets. Published results indicate that the precipitation of γ'' in Nb bearing alloys proceeds by homogeneous nucleation and growth in contrast to vanadium containing alloys in which transformation is initiated by "continuous ordering."[11]

As identified by Kirman,[7] equilibrium precipitation of β-Ni_3Nb in nickel and iron base alloys occurs via either of two discontinuous precipitation reactions. At low aging temperatures (≤973 K (700°C)) β forms through a classical cellular reaction initiating at the grain boundaries, while at higher temperatures (≥1073 K (800°C)) β forms predominantly as a transgranular Widmanstaetten precipitate on the {111} planes of the matrix. The crystallographic orientation relationship of the β phase with the matrix are similar for both the cellular and Widmanstaetten morphologies. The onset of the formation of the β phase corresponded to the initiation of softening during aging. Further work by Kirman and Warrington[8] revealed that it was possible to retard the discontinuous precipitation by alloying additions.

The present investigation was initiated to explore the strengthening of Cu-Ni alloys through the precipitation of γ''-Ni_3Nb particles and to study the precipitation sequence during aging. Based on the early work of C. S. Smith,[13,14] initial investigations were performed on two alloy compositions: Cu-30 pct Ni-1 pct Nb and Cu-30 pct Ni-2.5 pct Nb. Both optical and electron metallographic techniques were employed to follow the microstructural changes during aging.

EXPERIMENTAL PROCEDURE

Two ingots with nominal compositions of Cu-30 pct Ni-1 pct Nb and Cu-30 pct Ni-2.5 pct Nb were melted in an induction furnace under a flowing argon gas atmosphere and air cast by the Durville method. The ingots were homogenized for 2 h at 1227 K (950°C) and hot rolled from the same temperature to a gage of 0.0063 m (0.25 in.). Specimens for optical metallography and hardness testing were cold rolled to a gage of 0.00254 m (0.1 in.), and specimens for transmission microscopy were cold rolled to 254 μm (0.01 in.) gage.

The cold rolled specimens were homogenized for 1 h at 1372 K (1100°C) in an argon atmosphere and water quenched. Small coupons of the quenched specimens were encapsulated for subsequent aging treatment. Aging was performed at 866 K (600°C), 973 K (700°C), and 1073 K (800°C).

Specimens for transmission metallography were jet polished using a 30 pct nitric acid-methyl alcohol solution at 263 K. They were observed at 100 KV in an AEI EM-6G microscope.

EXPERIMENTAL RESULTS

Preliminary microstructural work revealed that after 2 h at 1372 K (1100°C) the alloy containing 1 pct Nb could be fully solutionized, while a fine dis-

M. RAGHAVAN is Engineering Specialist, Olin Corporation, Metals Research Laboratories, 91 Shelton Avenue, New Haven, CT 06511.

Manuscript submitted December 13, 1976.

persion of undissolved β-Ni_3Nb particles remained in the 2.5 pct Nb alloy. On aging the 2.5 pct Nb alloy showed higher peak hardness compared to the 1 pct Nb alloy and limited microscopy work on the 2.5 Nb alloy indicated that the precipitation sequence was essentially similar to the 1 pct Nb alloy. However, the undissolved β particles at the grain boundaries and in the grains interfered with the analyses of the precipitation during aging and, hence, further investigation on this alloy was discontinued. Only the results of the 1 pct Nb alloy are presented and discussed in this article.

Hardness

Figure 1 shows the aging response of the alloy on aging at 866 K, 973 K, and 1073 K for different aging times. Aging at 866 K produced a monotonic increase in the hardness of the alloy which levels off after 65 h. Overaging was not observed even at 200 h. At 973 K the alloy aged rapidly to attain peak hardness after 30 min. The hardness was maintained for 4 h and then decreased slowly up to 100 h which was the longest aging time examined at this temperature. Aging at 1073 K hardened the alloy within 5 min followed by rapid overaging. The maximum peak hardness was obtained at 866 K.

Metallography

Aging at 866 K (600°C). Optical metallography revealed no precipitation on aging up to 200 h. Electron microscopy studies of the alloy aged for 65 h showed fine, modulated structure indicating initiation of decomposition. However, individual precipitate particles could not be clearly resolved due to overlapping strain fields of the particles. Aging for 100 and 200 h caused very little coarsening of the particles, but it was possible to resolve the precipitates in bright field image by orientation contrast. Figure 2 is a bright field image of the γ'' precipitates after aging for 200 h. The precipitates formed as square platelets of the {100} matrix planes. Precipitation of β phase at the grain boundary was evident after 100 h with an attendant formation of a precipitate free zone (*PFZ*) with a width of 500Å. This width increased after aging for 200 h. Aging up to 200 h did not result in any cellular reaction or Widmanstaetten β precipitates.

Aging at 973 K (700°C). Decomposition of the supersaturated γ phase occurred after short aging times at 973 K. A modulated structure was observed after 10 min of aging, and bright field images on aging up to 75 min did not resolve the precipitates (Fig. 3). However, after 30 min weak superlattice reflections were observed at the locations corresponding to an ordered DO_{22} structure at (100) and (110) matrix reciprocal lattice positions; the former reflection

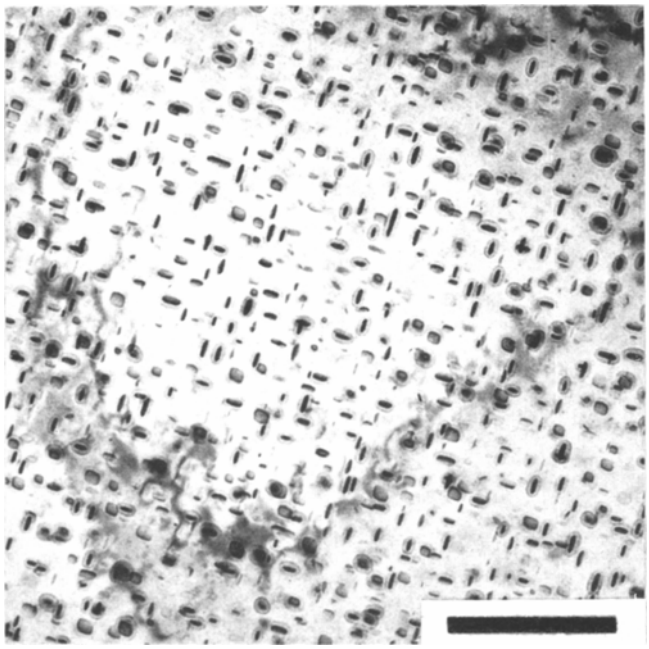

Fig. 2—Specimen aged at 866 K (600°C) for 200 h; bright field image showing fine γ'' particles. Marker denotes 0.15 μm.

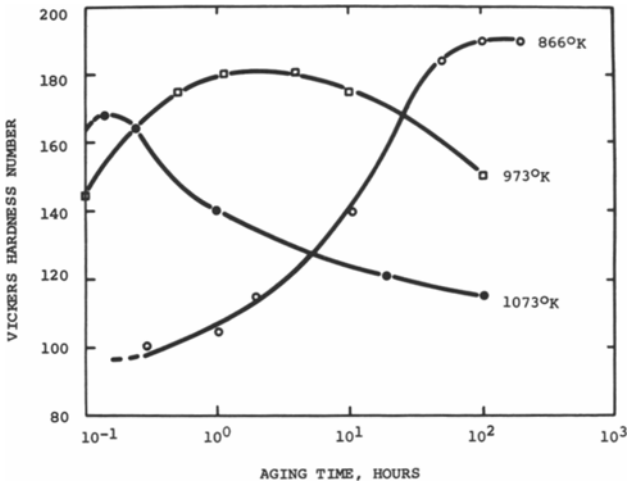

Fig. 1—Isothermal aging curves for specimens aged at 866 K, 973 K, and 1073 K.

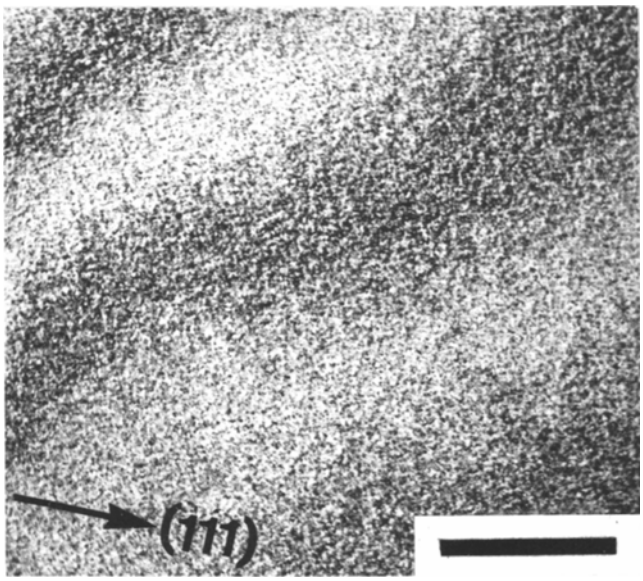

Fig. 3—Specimen aged at 973 K (700°C) for 75 min; bright field image showing modulated structure. Marker denotes 1 μm.

was streaked in the [100] direction, while the latter was not, and dark field imaging of the reflections indicated the formation of discrete ordered precipitates. Figure 4 shows these images for a specimen aged for 75 min, and it is clear that the dark field imaging of the (100) reflection revealed particles elongated along the [010] direction (Fig. 4(*a*)), while the (110) reflection imaged essentially equiaxed particles (Fig. 4(*b*)).

Aging for longer times caused considerable coarsening of the γ'' particles in the plane of the platelets. Figure 5(*a*) shows a bright field image at a [001] foil orientation showing all the three variants of the precipitate. The three precipitate variants, each having a DO_{22} superlattice, contribute to the selected area diffraction pattern shown in Fig. 5(*b*). The streaking of the $\{100\}$ and $\{1\frac{1}{2}0\}$ relpoints and absence of streaking of the $\{110\}$ relpoints are related to the shape factor of the precipitate variants.[1] The positive misfit between the precipitates and the matrix is readily evident from the diffraction pattern. The (100) and $(\frac{1}{2}10)$ reflections are displaced in the $[\bar{1}00]$ direction, while the (010) and $(1\frac{1}{2}0)$ reflections are displaced in the $[0\bar{1}0]$ direction towards the origin with reference to the fundamental reflections. This displacement is more evident in the higher order superlattice reflections as marked by arrows in Fig. 5(*b*). The γ'' precipitates are coherent even on aging for 100 h.

After aging for 4 h, a discontinuous cellular reac-

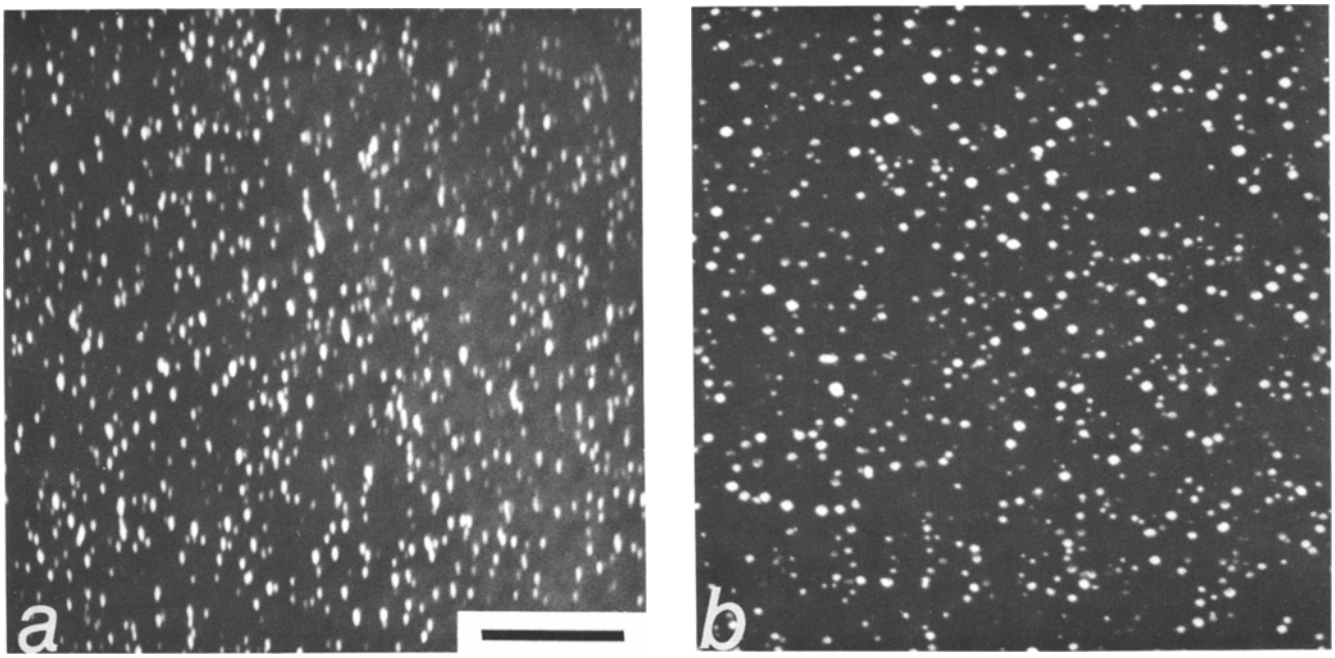

Fig. 4—Specimen aged at 973 K (700°C) for 75 min; dark field images of: (*a*) (100) and (*b*) (110) superlattice reflections. Marker denotes 0.2 μm.

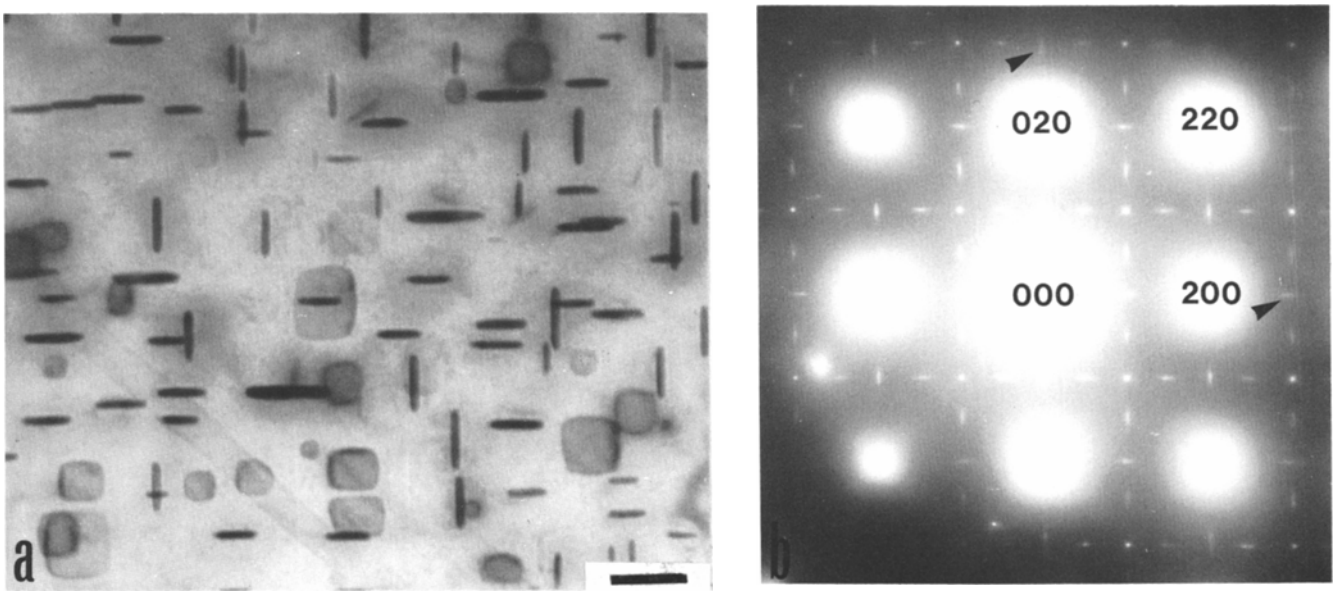

Fig. 5—Specimen aged at 973 K (700°C) for 65 h; (*a*) bright field image showing all three $\{100\}$ variants of γ'' and (*b*) [001] selected area diffraction pattern. Marker denotes 0.05 μm.

tion appeared at the grain boundaries. With increased aging time, the cellular product gradually grew into the grains at the expense of the γ'' precipitates, but reached only about 15 vol pct after 100 h. No evidence of the formation of Widmanstaetten β precipitates was noted even after 100 h of aging. Precipitation of β at grain boundaries and the formation of a *PFZ* was observed on aging for 4 h or longer. Figure 6 shows a typical grain boundary of a specimen aged for 65 h. The size of the γ'' precipitates in the matrix and in the *PFZ* boundary are comparable.

Kirman and Warrington[8] had indicated that the *PFZ* in Nb bearing nickel alloys could be either vacancy or solute depleted. In the present investigation, the *PFZ* seemed to be solute depleted since no preferential coarsening of the γ'' precipitates at the *PFZ* boundary was noted (Fig. 6). To ascertain the nature of the *PFZ* in the present system, a critical experiment was performed based on the earlier investigations of Embury and Nicholson[18] and Thomas.[19] Embury and Nicholson reported the use of double aging treatment to demonstrate the formation of vacancy depleted *PFZ* in aluminum alloys, and Thomas employed cold deformation prior to aging to combat the vacancy depleted *PFZ*. Combining both these approaches, a specimen was aged at 973 K for 65 h, cold rolled 15 pct, and aged at 866 K for 100 h. The microstructural examination of this specimen revealed that no additional precipitates formed in the *PFZ* confirming the indication that the *PFZ* was solute depleted.

Aging at 1073 K (800°C). Precipitation and growth of γ'' was extremely rapid at 1073 K and resolvable γ'' precipitates were observed within 5 min of aging. In the specimen aged for 4 h, the γ'' precipitates were considerably coarsened but remained coherent with the matrix. This is evident from the dark field image in Fig. 7 which shows interstitial strain contrast as was indicated by Ashby and Brown[20] and Thomas.[21] Also, frequent alignment of the γ'' precipitates and isolated instances of the formation of Widmanstaetten β (Fig. 8) were observed. Aging for 100 min was sufficient for the appearance of the cellular reaction at the grain boundary occupying less than 5 pct of the volume. The grain boundary cellular precipitate did not grow significantly on aging at 4 h but remained about 5 pct of the volume.

The microstructure after aging for 24 h was characterized by the formation of Widmanstaetten β platelets, and optical metallographic examination suggested that the grain boundary cellular precipitate also transformed to Widmanstaetten β. A transmission electron micrograph, Fig. 9, shows the formation of the β platelets on three $\{111\}$ variants of the matrix. The crystallographic analysis revealed the following relationship:

$$(010)_\beta // (111)_\gamma$$
$$[100]_\beta // [1\bar{1}0]_\gamma.$$

Presence of untransformed γ'' particles is also evident in Fig. 9.

Aging for 100 h transformed most of the γ'' precipitates to Widmanstaetten β (Fig. 10), and the volume fraction of the cellular precipitate was found to be less than 2 pct. At this aging time transformation of the cellular precipitate to Widmanstaetten β was more evident as shown in Fig. 11.

Measurement of misfit parameter normal to the platelets by electron diffraction showed that, within the accuracy of this technique, the parameter remained essentially constant at 1.8 pct over the entire spectrum of aging conditions investigated.

Particle Size

The size of the γ'' particles reported in this work arbitrarily refers to the length of the edge of the square platelets. At short aging times the measure-

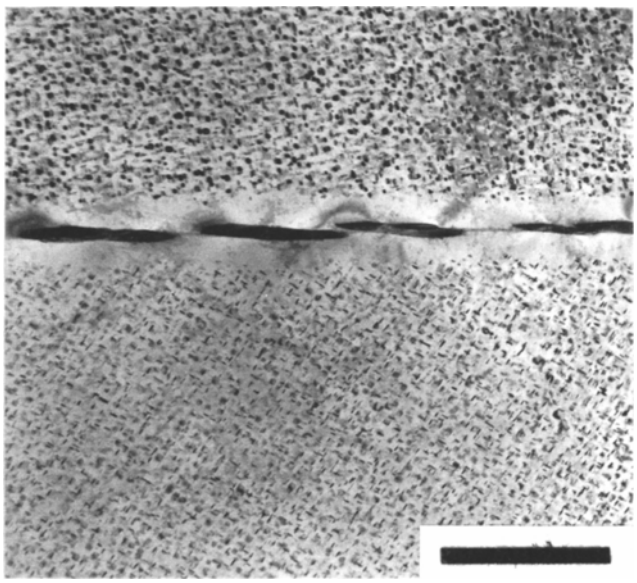

Fig. 6—Specimen aged at 973 K (700°C) for 65 h; bright field image showing the grain boundary β phase and the precipitate free zone. Note that the size of the precipitate at the *PFZ* boundary is comparable to the precipitates inside the grain. Marker denotes 1 μm.

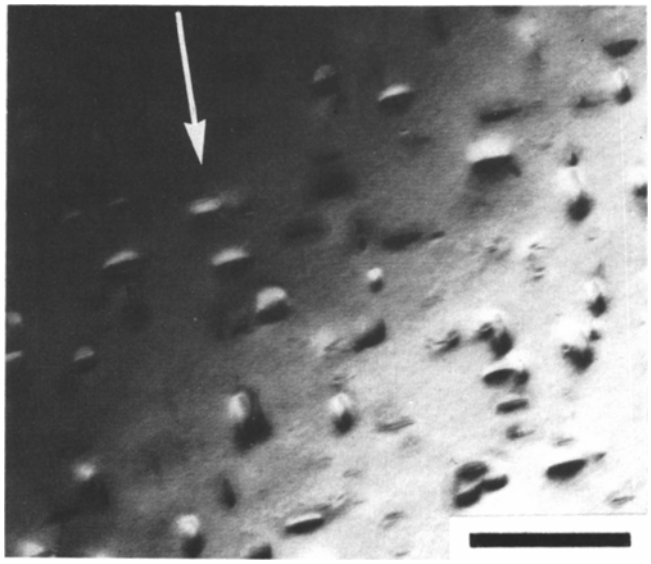

Fig. 7—Specimen aged at 1073 K (800°C) for 4 h; dark field image showing interstitial coherency strain contrast from γ'' precipitates. Arrow indicates the direction of positive (200) $\vec{g}$ vector. Marker denotes 0.5 μm.

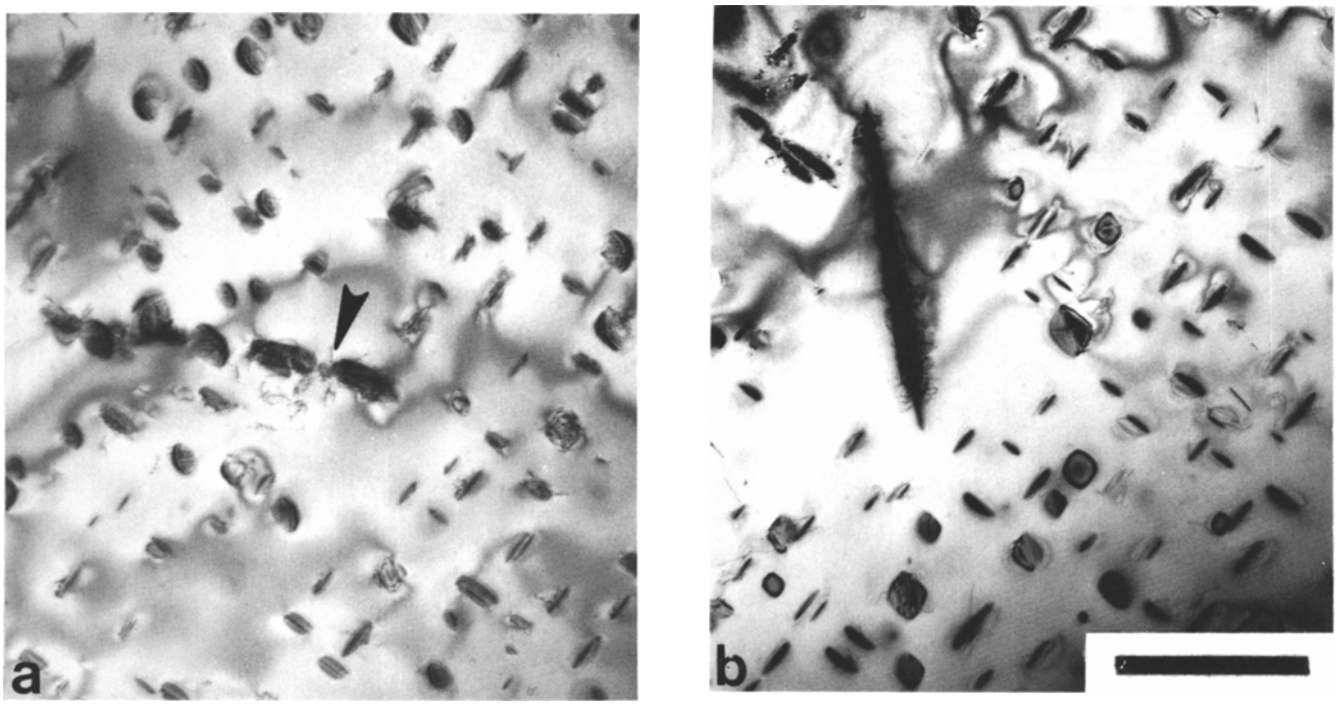

Fig. 8—Specimen aged at 1073 K (800°C) for 4 h; (*a*) bright field image showing alignment of particles (indicated by an arrow) leading to the formation of Widmanstaetten β phase as shown in (*b*). Foil orientation in (*b*) is [001]. Marker denotes 0.5 μm.

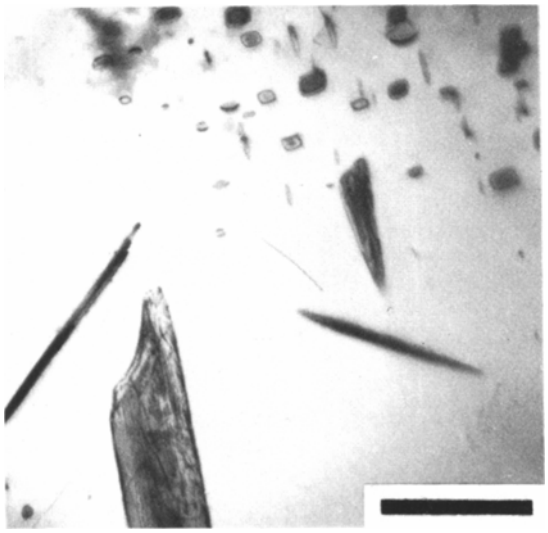

Fig. 9—Specimen aged at 1073 K (800°C) for 24 h; bright field image showing three {111} variants of Widmanstaetten β. Note presence of untransformed γ'' precipitates. Foil orientation [011]. Marker denotes 0.25 μm.

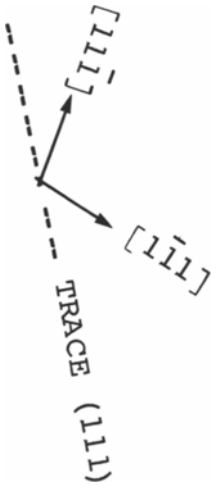

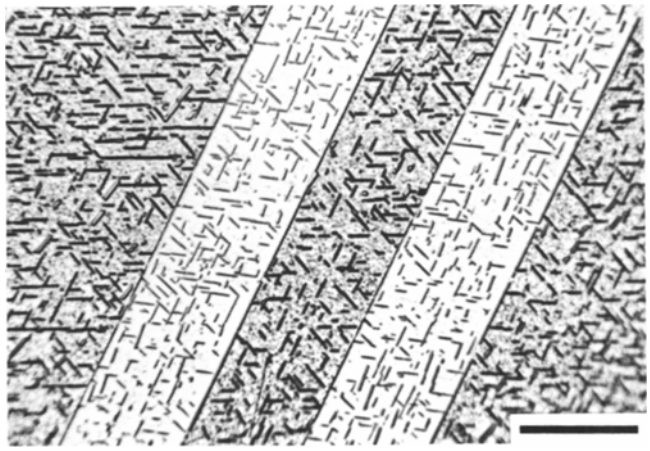

Fig. 10—Specimen aged at 1073 K (800°C) for 24 h; optical micrograph showing the formation of the Widmanstaetten β precipitates. Marker denotes 20 μm.

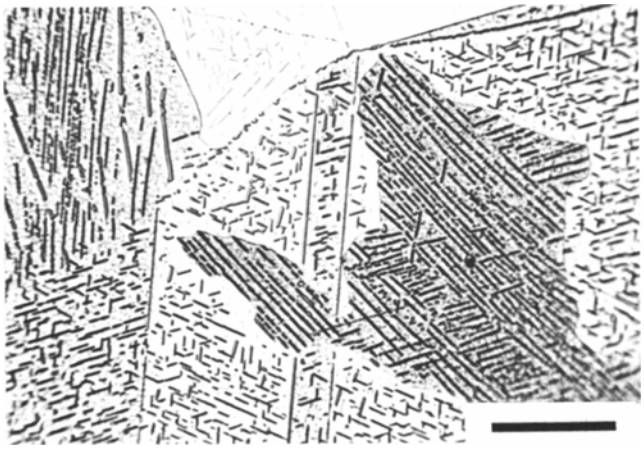

Fig. 11—Specimen aged at 1073 K (800°C) for 100 h; micrograph showing the transformation of the cellular β to Widmanstaetten β. Marker denotes 20 μm.

ments were made from dark field image using (100) superlattice reflections and at longer aging times when the individual particles could easily be resolved, the dimension was measured from the bright field image with the foil in a [001] orientation. In Fig. 12 the precipitate size is plotted as a function of (aging time)$^{1/3}$ at 973 K and 1073 K. The linear plots suggest that the coarsening follows a $t^{1/3}$ growth law, at least in the plane of the γ'' platelets. This observation is consistent with the work of Butler and Thomas[24] which suggested the applicability of Lifshitz-Wagner theory of volume diffusion controlled coarsening to nonspherical particles.

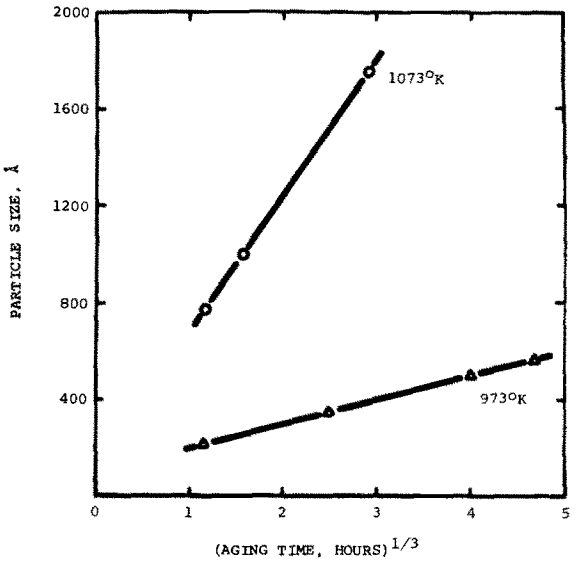

Fig. 12—(Aging time)$^{1/3}$ *vs* particle size plots for specimens aged at 973 K and 1073 K.

DISCUSSION

The preliminary microstructural investigations of Cu-30 pct Ni alloys containing 1 pct and 2.5 pct Nb indicated that the solid solubility of Nb at 1372 K (1100°C) is between these limits. Though the present investigation focused attention on the 1 pct Nb alloy, the 2.5 pct Nb alloy showed higher peak hardness on aging and improved grain growth resistance over 1 pct Nb alloy. These benefits are due to the higher volume fraction of γ'' precipitates and undissolved β precipitates at the grain boundaries, respectively.

Strength

There is little doubt that the hardening in the present alloy system is brought about by the precipitation of coherent Ni_3Nb-γ'' precipitates. Kirman[7] had pointed out that in Nb containing iron and nickel base alloys, overaging is due to the formation of the equilibrium β phase and not as a result of coarsening of coherent γ'' particles. This seems to hold good in the present alloy system. Aging at 866 K up to 200 h did not cause overaging or any detectable formation of the equilibrium phase. Softening on aging at 973 K was observed after 4 h and was accompanied by the formation of the cellular precipitate. Aging at 1073 proceeded so rapidly that sufficient metallographic data at short aging times are not available to confirm this explanation.

Peak hardness, as suggested by Kirman,[7] did not correspond to any definite γ'' particle size. At 973 K the peak hardness was maintained from 30 min to 4 h with the γ'' particle size changing from 100Å at 30 min to 275Å at 4 h. Similarly, there was no appreciable change in hardness values at 866 K when the particle size changed from less than 75Å at 65 h to 150Å at 200 h. Though overaging at 973 K was initiated by the cellular reaction, the gradual decrease in hardness after 24 h (Fig. 1) may be attributed in part to the coarsening of the γ'' precipitates since the cellular reaction proceeded only to 15 pct by volume after 100 h of aging.

Precipitation Sequence

The characteristics of the γ'' precipitation and the subsequent discontinuous reactions in the present investigation are similar to the observations made in nickel and iron base alloys.[1-11,16,17] This readily follows from the similarities in the lattice parameters of nickel, γ-iron, and copper which results in comparable γ''-matrix misfit values. It has been demonstrated that discrete ordered particles formed at very early stages of aging suggesting that the decomposition of the supersaturated solution occurs by homogeneous nucleation and growth. Also, the constancy of misfit parameter between γ and γ'' at 1.8 pct over the range of aging conditions investigated implies that the chemistry of the ordered precipitates does not change appreciably during aging.

The morphology of the equilibrium β precipitate depends on the aging temperature. At 866 K no β phase was observed up to 200 h. Aging at 973 K resulted in a limited proportion (about 15 vol pct) of the cellular product at least up to 100 h. This is consistent with a previous investigation of a niobium containing nickel base alloy where only 20 vol pct of the cellular precipitate was observed after 1000 h of aging at 973 K.[9] At 1073 K, the cellular precipitate formed at the grain boundaries up to 4 h, and aging for long times resulted in the formation of Widmanstaetten β. Major proportion of the Widmanstaetten β formed directly from the γ'', and a limited proportion of the Widmanstaetten β could have formed from the cellular precipitate. The preference for the formation of the cellular reaction compared to the formation of Widmanstaetten β at low aging temperatures was explained by Speich in terms of enhanced surface diffusion at low temperatures.[25] Widmanstaetten β formed at higher aging temperatures when bulk diffusion is significant. Based on these observations made in the present investigation, schematic transformation curves for the start of the transformations have been constructed for water quenched and aged specimens and are shown in Fig. 13. Solid and dotted lines indicate actual and projected data, respectively. At the aging temperatures investigated in this study, decomposition of the supersaturated γ phase always occurred through the formation of metastable γ'' precipitates. Since direct decomposition to the equilibrium β phase could possibly occur at temperatures higher than those examined here, this possibility is indicated in the dia-

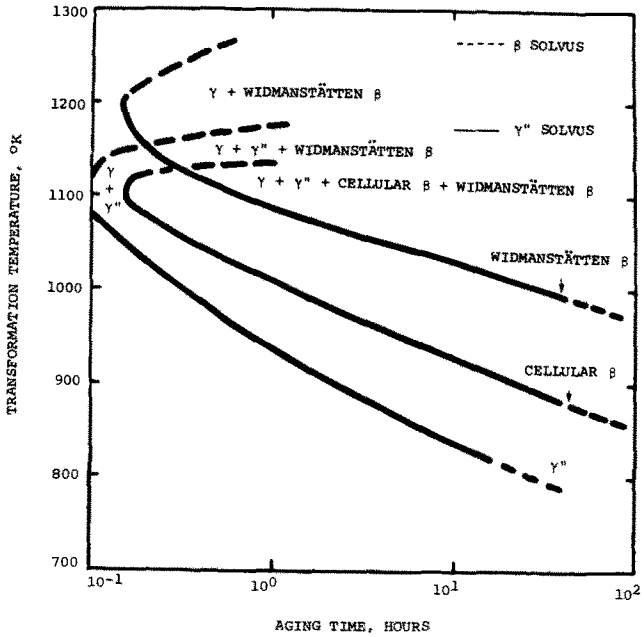

Fig. 13—Schematic transformation curves. Dashed lines indicate projected data.

gram. Detailed study of the transformation sequence above 1073 K is in progress and will be reported later.

Grain Boundary Precipitates and Precipitate Free Zone

The grain boundary precipitate in the present study was established to be the equilibrium β phase. In this respect, it differs from the carbon containing nickel and iron base alloy systems where precipitation of NbC and $M_{23}C_6$ at the grain and twin boundaries were observed. The experimental results indicated that the *PFZ* formed was solute and not vacancy depleted. This difference in the origin of the *PFZ* is evident comparing the γ'' precipitate size at the *PFZ* boundary. In the present study the precipitate size at the *PFZ* boundary was comparable to matrix precipitates, while structural observations by Kirman and Warrington[9] indicated coarser precipitates at the zone boundary compared to the matrix (Fig. 8 of Ref. 9). Thus, it is suggested that the *PFZ* formed in the present alloy system is solute and not vacancy depleted. The effect of this solute free *PFZ* on the mechanical properties of the alloy is not yet known.

Though the exact mechanism by which the Widmanstaetten β forms from γ'' precipitate is not clear, it appeared (Fig. 8) that the early stages of formation of β was characterized by the alignment of γ'' particles with *in situ* transformation to the Widmanstaetten β platelets. In their work on Ni-Fe-Cr-Nb alloys, Kirman and Warrington suggested that this preferential alignment of the γ'' particles could result from the extrinsic stacking faults observed in the γ phase.[9] Since no stacking faults were observed in the present study, the reason for alignment of γ'' particles is not clear. They also suggested that faulting within the γ'' precipitates during their growth could act as potential nucleation sites for the Widmanstaetten β phase. Earlier work by Merrick and Nicholson in a Ni-Cr-Ti alloy showed definite evidence of condensation of vacancies resulting in intrinsic faults in particles prior to transformation to the equilibrium η hcp phase.[22] Though a similar mechanism is feasible in the γ'' to β transformation in the present study, due to similarity between hcp (η) and orthorhombic (β) structures, no direct evidence of this mechanism was obtained. The γ'' particles that aligned to form subsequent β particles showed no fringe contrast and no other evidence of faulting; *e.g.* streaking along $[112]_{\gamma''}$ direction was not observed as would be expected if faulting were present.[9]

CONCLUSIONS

1) Age hardening observed in the Cu-30 pct Ni-1 pct Nb alloy system was the result of the precipitation of ordered, coherent, metastable Ni_3Nb-γ'' precipitates which formed by homogeneous nucleation and growth. Coarsening of the γ'' precipitates followed a $t^{1/3}$ growth law in the plane of the precipitates.

2) Equilibrium β phase formed through a grain boundary cellular reaction at low aging temperatures ($\leq$973 K) or Widmanstaetten precipitates at higher aging temperatures ($\geq$1073 K).

3) Grain boundary precipitation during aging was associated with a solute depleted precipitate free zone.

ACKNOWLEDGMENTS

The author would like to thank Dr. R. N. Caron for helpful discussions and suggestions during the course of the investigation. Special thanks are due to Ms. S. Barnes for help in preparing the manuscript, Mr. C. Steineck for help in preparing thin foils, and Dr. E. Shapiro and Mr. J. Crane for encouragement during the work. This work was supported by the Olin Brass Group.

REFERENCES

1 J. M. Oblak, D F Paulonis, and D S. Duvall. *Met. Trans.*, 1974, vol. 5, pp. 143-53.
2. H J. Wagner and A M Hall *Physical Metallurgy of Alloy 718*, DMIC, Report 217, 1965
3 P S. Kotval *Trans. TMS-AIME*, 1968, vol. 242, pp. 1764-65
4 D F Paulonis, J. M Oblak, and D. S Duvall *Trans. ASM*, 1969, vol. 62, pp 611-22.
5 M. V. Nevitt *Electronic Structure and Alloy Chemistry of Transition Elements*, P A. Beck, ed , p. 169, Interscience Publishers, New York, 1963.
6 R Cozar and A Pineau: *Met. Trans* , 1973, vol. 4, pp. 47-59.
7 I. Kirman *J. Iron Steel Inst.*, 1969, vol. 207, pp. 1612-18.
8. I Kirman and D H. Warrington *J. Inst. Metals*, 1971, vol. 99, pp. 197-99.
9 I. Kirman and D H. Warrington *Met. Trans.*, 1970, vol 1, pp. 2667-75.
10 R. T. Weiner and J J. Iram: *Trans. ASM*, 1966, vol 59, p 340
11. H. A Moreen, R Taggart, and D H. Polonis *Metallogr* , 1974, vol 7, pp. 513-21.
12 D. H Roach, R B. Fischer, and J H Jackson. *Trans ASM*, 1954, vol. 46, pp 329-47.
13 R. Knights and P. Wilkes *Acta Met.*, 1973, vol 2, pp 1503-14.
14 C S Smith. U.S Patent 2,430,603 (1947).
15 C S. Smith. British Patent 569,408 (1945)
16. I. Kirman and D H. Warrington *J. Iron Steel Inst* , 1967, vol. 205, pp. 1264-65.
17. I. J. Polmear *J. Austral. Inst. Met* , 1966, vol. 11, p. 246

18. J. D. Embury and R. B. Nicholson: *Acta Met.*, 1965, vol. 13, pp. 403–17
19. G. Thomas: *J. Inst. Metals*, 1960–61, vol. 89, pp. 287–88.
20. M. F. Ashy and L. M. Brown *Phil. Mag.*, 1963, vol. 8, pp. 1083–103; 1649–76.
21. G. Thomas *Modern Diffraction and Imaging Techniques in Material Science*, pp. 131–58, North-Holland Publishing Company, 1970
22. H. F Merrick and R B. Nicholson Proc. 5th International Conference on Electron Microscopy, K8, 1962.
23. H. T. Michels, I. B. Cadoff, and E. Levine: *Met. Trans.*, 1972, vol. 3, pp. 667–74.
24. E P. Butler and G Thomas. *Acta Met*, 1970, vol. 18, pp. 347–65.
25. G. R. Speich *Trans. TMS-AIME*, 1963, vol. 227, pp. 754–62.